Journal of Simulation and Analysis of Novel Technologies in Mechanical Engineering
17 (4) (2025) 0059~0070
DOI 10.71939/jsme.2025.1213979

Research article

Numerical simulation of pool boiling heat transfer using silica-water, copper oxide-water, and aluminum oxide-water nanofluids on a vertical brass cylinder

Yaser Seyfipour[1], Shoeib Mahjoub[1], Saeed Daneshmand[1], Esmaeil Abedi[2]*

[1]*Department of Mechanical Engineering, Is.C., Islamic Azad University, Isfahan, Iran*
[2]*Department of Mechanical Engineering, Shahi.C., Islamic Azad University, Shahinshahr, Iran*

*esmaeil.abedi@iau.ir

(Manuscript Received --- 04 Aug. 2025; Revised --- 29 Oct. 2025; Accepted --- 09 Dec. 2025)

Abstract

Heat transfer in fluids is of great importance. There are several methods to improve heat transfer. One of these methods is the use of nanofluids. Given the widespread use of brass metal in nuclear reactor cores, water-cooled electronic devices, and refrigeration systems and equipment, this research aims to improve heat transfer, increase the convective heat transfer coefficient, and increase the heat flux compared to pure water by numerically simulating the heat transfer of a brass cylinder immersed in a fluid-filled pool. For this purpose, after modeling the geometry, with the help of software ANSYS Fluent (v. 2022 R1), meshing is performed for the modeled geometry, and by applying the conservation equations and energy, and applying the properties and initial and boundary conditions, the heat transfer time and thermohydraulic properties of the problem are obtained. The base fluid used is pure water, which has been converted into a nanofluid by adding silica nanoparticles, copper nanoparticles, and aluminum nanoparticles to it. New properties obtained from the combination of base fluid and nanoparticles with any volume fraction have been introduced into the software. In this research, first, simulation is performed with the properties of the base fluid (pure water), then simulation is performed with the properties obtained for each of the volume fractions of nanofluids. The simulation results show that the heat transfer of the nanofluid has changed compared to pure water, such that at small volume fractions (0.05), the results show less growth, but at volume fractions (0.1 and 0.15), the results show a growth of over 15%, but in the silica water nanofluid at a density of (0.05), better heat transfer occurs.

Keywords: Numerical simulation, nanofluid, brass cylinder, different concentrations, Heat transfer.

1- Introduction

Improving heat transfer has always been an important and discussed issue in industry. This increase is used in many heat transfer phenomena such as electronic chips, laser systems, power plants, spacecraft, air conditioning systems, foundries and other industrial equipment. With the advancement of science and technology, significant steps have been taken in the operation and efficiency of heat transfer equipment. The most important heat transfer parameters that are most concerned include increasing heat flux, heat transfer coefficient and optimal dimensions of the equipment. There are different methods for improving thermal efficiency, among which the use of expanded surfaces (fins) or roughening of heat transfer surfaces can be mentioned. In recent years, studies have been conducted on different shapes, dimensions and materials in heat transfer of nanofluids, but today, due to the widespread use of brass metal in various industrial applications and places where there is practically no need to exchange heat with an intermediate fluid, and according to past research, several nanofluid samples including silica-oxide water, copper oxide water and aluminum oxide water were used in this work. Studies have also been conducted on the effect of different nanofluids on different metals, each of which has been used in different devices.

Sheikhzadeh et al. [1] numerically investigated the effect of water-aluminum oxide and water-copper nanofluids on heat transfer in a copper shell and tube heat exchanger. Their results show that adding nanoparticles to the base fluid increases heat transfer. Kersi and Kim [2] conducted an experimental study of the effect of nanofluids on the surface during boiling. The results show that the presence of nanofluids at a concentration of 0.001 does not change much on the surface and heat flux, but a concentration of 0.5 causes a 37% increase in heat flux and changes in the surface. Kim et al. [3] have conducted experimental studies on the heat removal process on stainless steel spheres and zirconium spheres. These objects have been exposed to pure water and base water and small droplets of aluminum, silica and diamond nanoparticles at low concentrations (less than 0.1% by volume). Their results show that the presence of nanofluids in initial tests is close to the results of pure water. Jahanshahi et al. [4] studied numerical simulation of free flow based on thermal conductivity measurements in a square cavity using silica water nanofluid and concluded that increasing the volume fraction does not change much in increasing Nusselt and heat transfer, while in laboratory work, significant changes were observed, which they attributed to the deposition of nanoparticles. In another study, plasma spray coating was investigated to increase the heat transfer coefficient and CHF value [5]. In this work, three plasma coated aluminum surfaces (C-15, C-20, and C-25) were fabricated on a copper substrate with three different plasma powers of 15, 20, and 25 kW, respectively, and the pool boiling heat transfer was analyzed. The results of this work show that the plasma coated surfaces have improved absorption and wettability properties compared to the plain copper surface. Another study investigated methods for increasing pool boiling heat transfer on horizontal tubes [6]. The results of this study showed that surface roughness can increase the nucleation site density by up to 67.5%, the heat transfer coefficient by up to 17%, the HTC by 400%, the critical heat flux by more than 100%, and the heat transfer efficiency significantly. Another study conducted experiments on four welding surfaces in the pool welding process [7]. The aim of this study was to find the optimal surface configuration that can effectively absorb the maximum heat flux while minimizing the temperature difference. The results of this study indicate that unidirectional polished surfaces with low roughness perform better in critical heat flux compared to surfaces with circular roughness, and the proposed modifications result in a significant increase of 131% in CHF and a significant increase of 211% in heat transfer coefficient (HTC). In the field of the effects of nanoparticle migration on the natural convection behavior of nanofluids, research has been conducted to analyze a hybrid model by considering important phenomena such as Brownian motion and thermophoresis effects [8]. In this work, the governing equations have been solved numerically and the results have been confirmed by experimental observations. The results show that the assumption of single-phase nanofluid for natural convection is not accurate enough and the flow behavior for natural convection of nanofluids is different from the base fluid. In this work, the effects of thermophoresis parameter, volume fraction and diameter of nanoparticles on the flow behavior and heat transfer have also been investigated.

Study of carbon nanotubes and the factors affecting the pool boiling heat transfer coefficients (HTC) and critical heat flux (CHF) have been studied in another study [9]. For this purpose, three nanofluids including CNT treated with GA, cysteine and Ag at different weight concentrations were used and their thermal performance was investigated. The results of this study show that while the pool boiling HTC of non-covalent nanofluids was lower than that of deionized water, the covalent nanofluids show a significant increase and with decreasing CNT size, the specific surface area increases, indicating higher CHF and HTC. In the field of nanofluids, a study has been conducted to study the performance of a conical spiral heat exchanger [10]. In this work, rectangular sections have been investigated using aluminum oxide/water (Al2O3/water) and copper oxide/water (CuO/water) nanofluids. The effects of nanofluid concentration on secondary flow, pressure drop, heat transfer, and factor of merit (FOM) have also been investigated. The results show that increasing the nanofluid concentration causes the secondary flow to gain more strength and reduce the heat transfer rate. In addition to nanofluids, nanofluids can be used in airflow studies, including studies on the effect of wind tunnel specimens on aerodynamic properties [11]. In such studies, nanofluids can be used instead of air and the effect of the model on fluid flow along with heat transfer can be investigated.

Understanding the behavior and characteristics of heat transfer on different metals will improve the performance of systems and increase their efficiency [12]. A review of previous studies indicates that most investigations on boiling heat transfer using nanofluids have been conducted under controlled laboratory conditions, typically employing substrates made of metals other than brass. However, in many cases, the exact substrate material is not explicitly specified [13]. Among the applications of brass metal in industry are systems made of brass metal that exchange heat with an intermediate fluid such as water. Heat exchangers of electronic devices and refrigeration devices are examples of these. In this research, the heat transfer of a brass cylinder immersed in different nanofluids with different concentrations is investigated. For this purpose, the governing equations of the problem are first examined. These equations include the continuity equation, the momentum equation, the energy equation, and the nanofluid equations. The continuity, momentum, and energy equations are discretized in three dimensions in cylindrical coordinates. Then, these equations are solved using Fluent software.

2- Governing equations

The equations used in this work are as follows [14].

Continuity equation:

$$\frac{D\rho}{Dt} + \rho\nabla.\boldsymbol{V} = 0 \qquad (1)$$

where ρ is the fluid density $\left(kg/m^3\right)$, $\frac{D\rho}{Dt}$ is the material derivative of density representing its rate of change following a fluid particle, $\nabla.\boldsymbol{V}$ is the divergence of the velocity field $\boldsymbol{V}\left(m/s\right)$, and $\boldsymbol{V}$ is the local velocity vector of the fluid.

Momentum equation:

$$\rho\frac{D\boldsymbol{V}}{Dt} = -\nabla P + \mu\nabla^2\,\boldsymbol{V} + \boldsymbol{F} \qquad (2)$$

where $\frac{D\boldsymbol{V}}{Dt}$ is the material derivative of the velocity vector $\boldsymbol{V}$, ∇P is the pressure gradient $\left(Pa/m\right)$, μ is the dynamic viscosity $\left(Pa.s\right)$, $\nabla^2\boldsymbol{V}$ is the Laplacian of velocity representing viscous diffusion, and $\boldsymbol{F}$ denotes the external body force per unit volume $\left(N/m^3\right)$.

Energy equation:

$$\rho\, cp \frac{dT}{dt} = k\nabla^2\, T + \psi \tag{3}$$

where c_p is the specific heat capacity at constant pressure $(J/kg.K)$, T is the temperature (K), t is time (s), k is the thermal conductivity $(W/m.K)$, $\nabla^2 T$ is the Laplacian of temperature representing spatial diffusion, and ψ is the internal volumetric heat generation rate (W/m^3).

Nanofluid density:

$$\rho_{nf} = (1-\phi)\rho_f + \phi\, \rho_s \tag{4}$$

where ρ_{nf} is the density of the nanofluid (kg/m^3), ρ_f is the density of the base fluid (kg/m^3), ρ_s is the density of the solid nanoparticles (kg/m^3), and ϕ is the volume fraction of nanoparticles (dimensionless).

Specific latent heat coefficient of nanofluid:

$$c_{pnf} = \frac{\phi(\rho_s\, c_{ps}) + (1-\phi)(\rho_f\, c_{pf})}{\rho_{nf}} \tag{5}$$

where c_{pnf} is the specific heat capacity of the nanofluid $(J/kg.K)$, c_{ps} and c_{pf} are the specific heat capacities of the solid and fluid phases respectively $(J/kg.K)$.

Nanofluid conductive heat transfer:

$$K_{nf} = \frac{K_S + 2\,K_f - 2\phi\,(K_f - K_S)}{K_S + 2\,K_f + \phi(K_f - K_S)} \tag{6}$$

where K_{nf} is the thermal conductivity of the nanofluid $(W/m.K)$, K_s is the thermal conductivity of the solid nanoparticles $(W/m.K)$, K_f is the thermal conductivity of the base fluid $(W/m.K)$.

3- Geometry of the problem

In this work, ANSYS Fluent (v. 2022 R1) software was used for numerical analysis. The geometry of the problem was drawn with the help of Gambit software, considering the details and locations. The part under study is a cylindrical tube with a diameter of 20 mm and a height of 75 mm, and the heat dissipation container in which the part is placed is 100 mm in diameter and 200 mm in height, as shown in Figure 1. In this simulation, the container is fabricated from Pyrex, modeling adiabatic boundary conditions with no heat exchange to the surroundings. The main dimensions of the cylinder geometry are: Ø20 mm × 75 mm height; chamber: Ø100 mm × 200 mm height. The container is considered insulated, the fluid inside the container (base fluid or nanofluid) has a saturation temperature (100 degrees), and the solid cylinder is made of brass and is assumed to be at a temperature of 600 degrees Celsius. These conditions are shown in Figure 2. Table 1 shows the thermophysical properties of the nanofluids used in this work and the base fluid (pure water) [15].

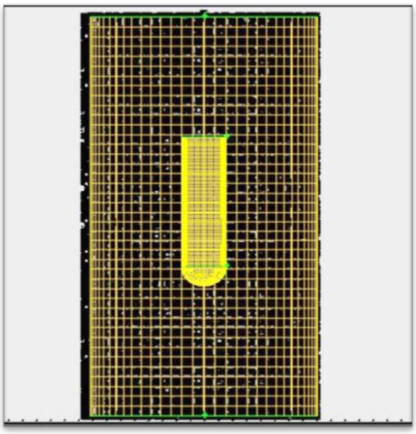

Fig. 1 Problem geometry

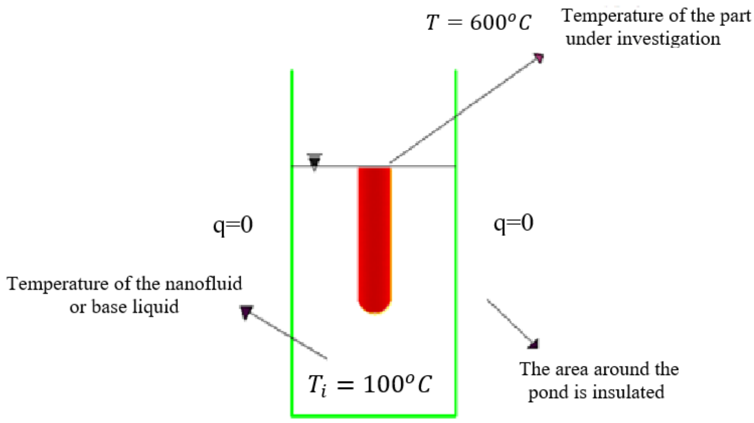

Fig. 2 Boundary and initial conditions of the problem

Table 1: Thermophysical properties of nanofluids and base fluid

Fluid	ρ (kg/m^3)	c_p $(j/kgc^{\circ}$	$k_{(w/mc^{\circ})}$
Silica nanoparticles	2220	745	1.38
Aluminum oxide nanoparticles	3880	773	2.37
Copper oxide nanoparticles	8940	401	3.85
Base fluid (pure water)	997.1	4175	00.613

4- Network independence

In order to make the numerical solution results independent of the grid, the solution domain is considered as follows. First, the results for pure water were obtained with the initial grid. Then the grid was halved and the results were obtained. Now this was repeated so that no change was observed in the results. In this simulation, high accuracy in independence from the grid was considered. Therefore, changes in node 92, which is one of the middle nodes of the section under study, were considered. Table 2 shows the results of changing the number of grid points. In this table, the number of grid points indicates the total number of computational points in the numerical domain, the time of the last heat transfer (seconds) indicates the time when the last noticeable temperature change occurred at node 92, and the temperature of the last heat transfer (degrees Celsius) is the temperature value recorded at that time.

Table 2: Change in network change ratio results

Last heat transfer temperature (Celsius)	Last heat transfer time (seconds)	Network points
240	130	10000
240	140	45000
240	110	65000
240	125	150000
240	125	230000

5- Solution method

To solve the problem, after drawing the geometry and meshing with the help of software, the data is entered into the ANSYS software. Then, the boundary conditions, initial conditions, and thermophysical properties of the test piece and the nanofluid with the desired concentration, as well as the base fluid, were entered into the software. In the following, the mesh independence process was considered for one of the conditions. For this purpose, the pure water condition was considered as the default. Finally, calculations were performed for nanofluids with each volume fraction in the same way by applying their properties and the results were obtained.

6- Analysis and review

Figure 3 shows the graph of the change in the temperature of the center of the rod in pure water in numerical simulation and the temperature of the center of the rod in pure water in laboratory work. Initially, the nuclear boiling process occurs and stable vapor formation occurs on the surface. In the simulation, this process takes longer in the sudden changes of the unstable vapor film, and the sudden changes pass through nuclear boiling and finally continue as a single phase. As can be seen from this figure, the simulation result is in good agreement with the experimental result. As is clear from this figure, in the simulation, at the beginning, the heat dissipation process decreases in temperature and continues with the same difference until the temperature approaches 300°C, which is essentially the stage where bubble production occurs around the part, and after passing this stage, as is clear from the experimental results, the temperature changes abruptly. This occurs at time 120 s, while in the simulation this sudden temperature change occurs slightly earlier than in the laboratory work, which is about (s) 125. The reason for this difference of (s) 5 in the simulation work compared to the laboratory work is the conditions of the laboratory environment.

7- Simulation results of water and various nanofluids

Using the nanofluid relationships and the thermophysical properties of nanoparticles and the base fluid, the properties of different nanofluids with different volume fractions (0.1%, 0.05%, and 0.15%) are obtained, which are listed in Tables 3, 4, and 5 for the thermophysical properties of nanofluids with different concentrations.

Table 3: Thermophysical properties of silica nanofluid for different volume fractions

ϕ (%)	ρ_{nf} $(kg/m)^3$	c_{pnf} $(j/kg\ c^{\circ})$	k_{nf} (w/mc°)
0.1	2097	858	0.993
0.05	2158	801	0.995
0.15	2036	914	0.910

Table 4: Thermophysical properties of aluminum nanofluid for different volume fractions

ϕ (%)	ρ_{nf} $(kg/m)^3$	c_{pnf} $(j/kg\ c^{\circ})$	k_{nf} (w/mc°)
0.1	3591	802	0.904
0.05	3735	787	0.951
0.15	3447	817	0.859

Table 5: Thermophysical properties of copper nanofluid for different volume fractions

ϕ (%)	ρ_{nf} $(kg/m)^3$	c_{pnf} $(j/kg\ c^c)$	k_{nf} (w/mc°)
0.1	8145	407	0959
0.05	8542	404	0.924
0.15	7748	410	0.834

Simulations were performed using the results obtained from thermophysical properties and software for each volume fraction and pure water.

Figure 4 shows the temperature contour and heat transfer process of the brass cylinder for pure water in numerical simulation. During heat transfer, the temperature of the part and the surrounding fluid changes greatly. Additionally, during the final stages the body approaches thermal equilibrium with the fluid. Also, in the last moments when the body reaches near isothermally with the fluid, there is heat accumulation at the bottom of the container and in the corners of the container up to the middle of the container body, and as mentioned earlier, this is due to the curved geometry of the bottom of the part, which causes the majority of heat to move from the bottom of the part.

As is clear from the stages of heat dissipation of the cylinder and the thermal gradient of the part, initially the heat is taken from the surrounding area of the part and it is at this stage that steam production occurs around the cylinder. This steam production around the part causes a sudden decrease in the temperature around the part and after the temperature around the part becomes lower than the center of the part, the temperature decrease starts from the bottom of the part and then the temperature decrease continues from the bottom of the part towards the top of the center of the part. Eventually, all parts of the part lose their heat. In general, the heat transfer behavior in all fluids used is similar to this case.

Figures 5 to 7 show the results of comparing the convective heat transfer coefficient in different nanofluids at uniform concentration for all volume fractions of nanofluid and base fluid (pure water).

As was obtained in the study of the convective heat transfer coefficient results, the results of low volume fraction (0.05) in the convective heat transfer coefficient diagram do not change significantly compared to the simulation results of pure water, which could be due to the deposition of nanoparticles on the part. This has caused the nanofluid results to be the same as pure water. At higher concentrations (0.1 and 0.15), more favorable results have been obtained compared to pure water.

Figures 8, 9, and 10 show the results of comparing heat flux (the centerline of the cylinder along the z-axis from z=0 to z=75 mm) in different nanofluids at uniform concentration for all volume fractions of nanofluid and base fluid (pure water).

As can be seen in the results obtained, the results of low volume fractions (0.05) in the heat flux change diagram do not change significantly compared to the results of pure water simulation. The heat flux values for pure water were higher than those for the nanofluid at low concentration (0.05), which can be attributed to nanoparticle deposition on the body surface increasing thermal resistance. However, at higher concentrations of nanofluid, the heat flux changes significantly. As expected, increasing the concentration has increased heat transfer. At low concentrations, the behavior of silica nanofluid has a higher heat flux than other nanofluids at a certain distance, indicating that the presence of more nanoparticles with a higher thermal conductivity in the base fluid does not always increase heat transfer.

The presence of nanofluid with a small volume fraction causes a negligible change in heat flux compared to pure water under simulated conditions, which is due to the deposition of bulk nanoparticles on the part.

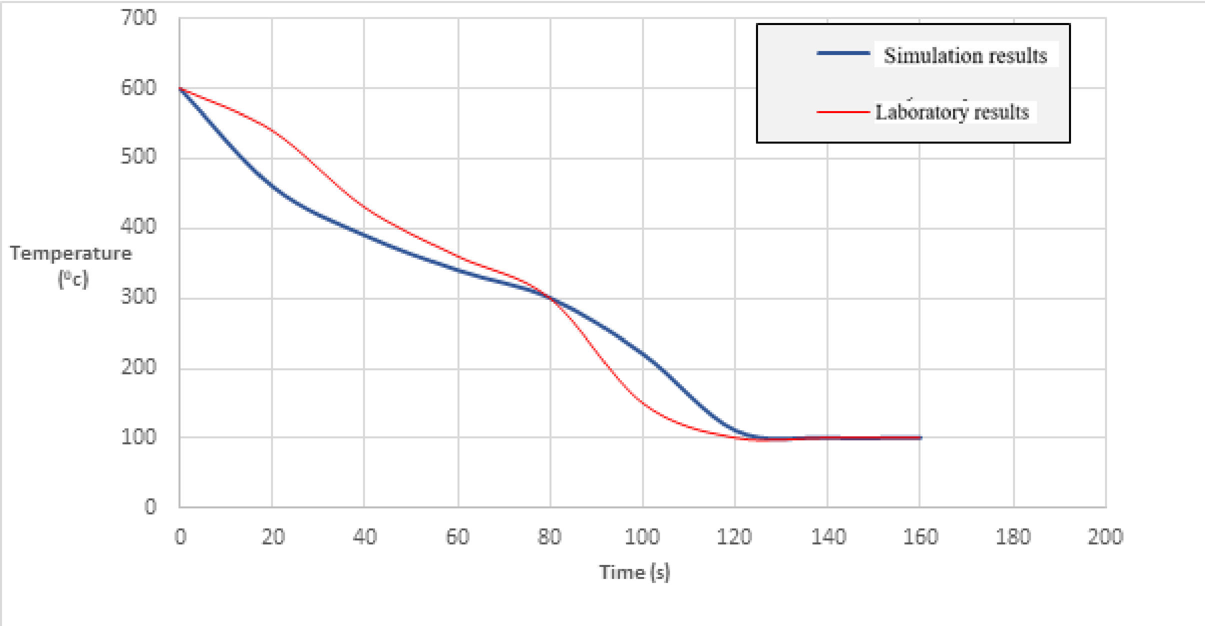

Fig. 3 Pure water results in simulation and experimental work [16]

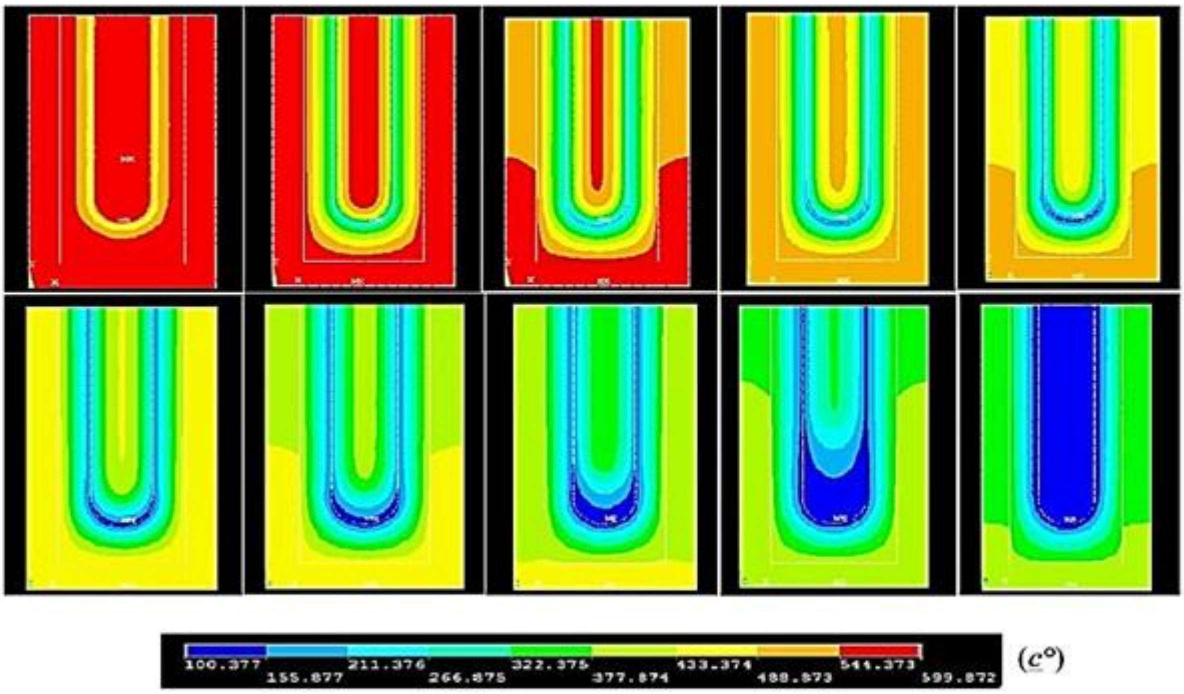

Fig. 4 Temperature contour of brass cylinder for pure water

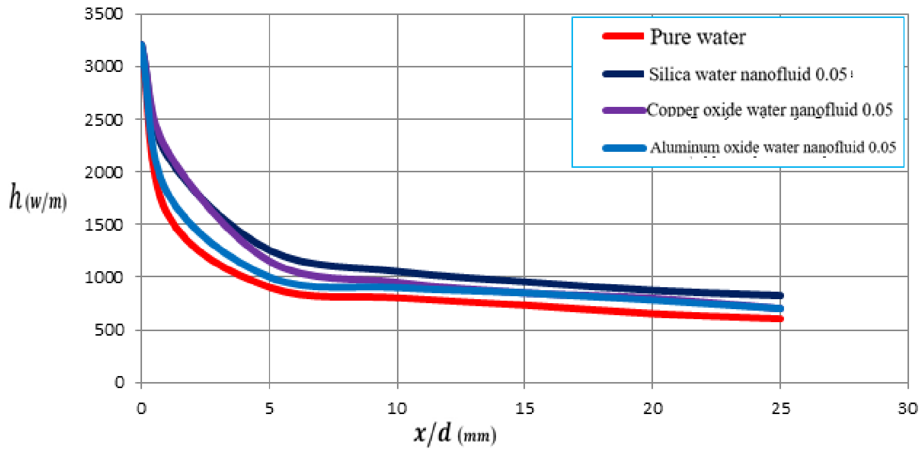

Fig. 5 Convection heat transfer coefficient for 0.05% volume concentration of all nanofluids and base fluid (pure water)

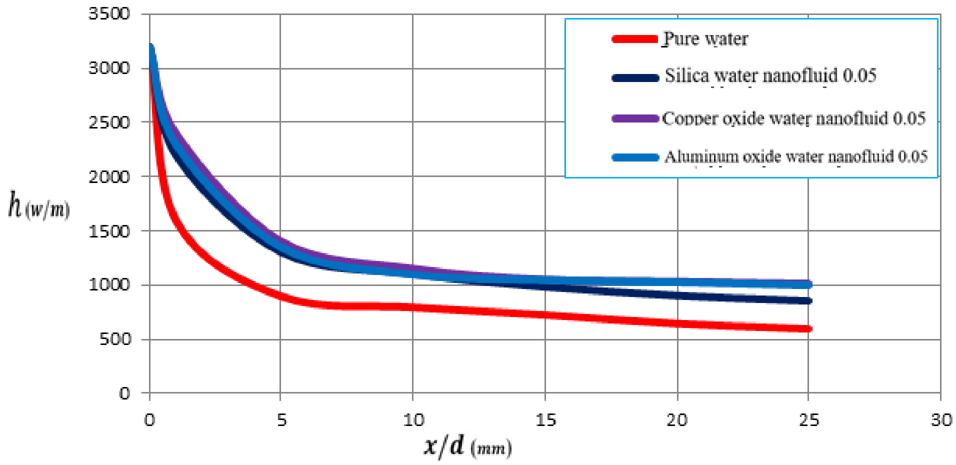

Fig. 6 Convection heat transfer coefficient for 10% volume concentration of all nanofluids and base fluid (pure water)

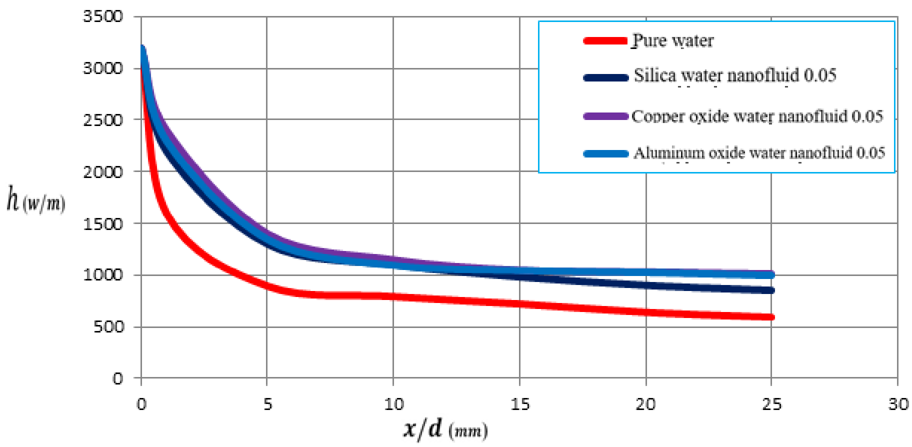

Fig. 7 Convection heat transfer coefficient for 15% volume concentration of all nanofluids and base fluid (pure water)

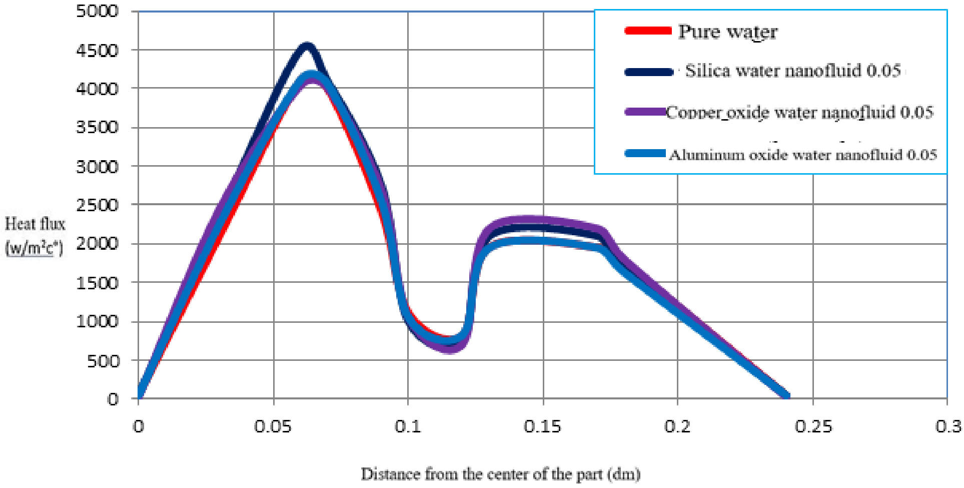

Fig. 8 Heat flux for 5% volume concentration of all nanofluids and base fluid (pure water)

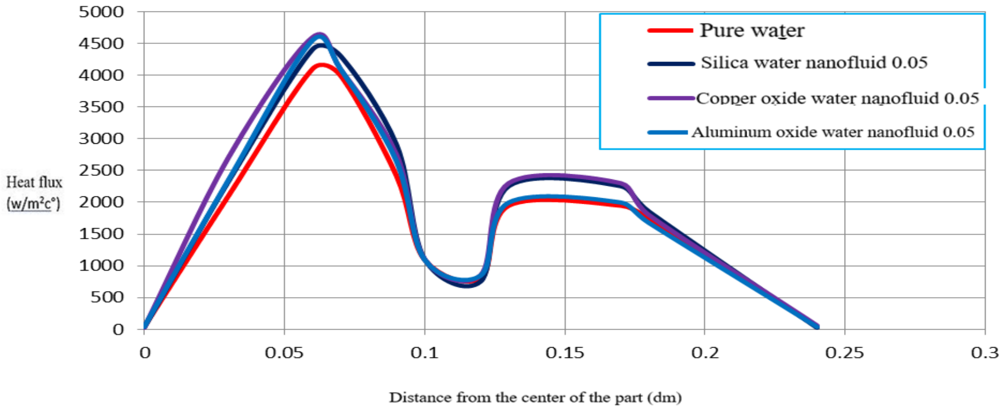

Fig. 9 Heat flux for 0.1% volume concentration of all nanofluids and base fluid (pure water)

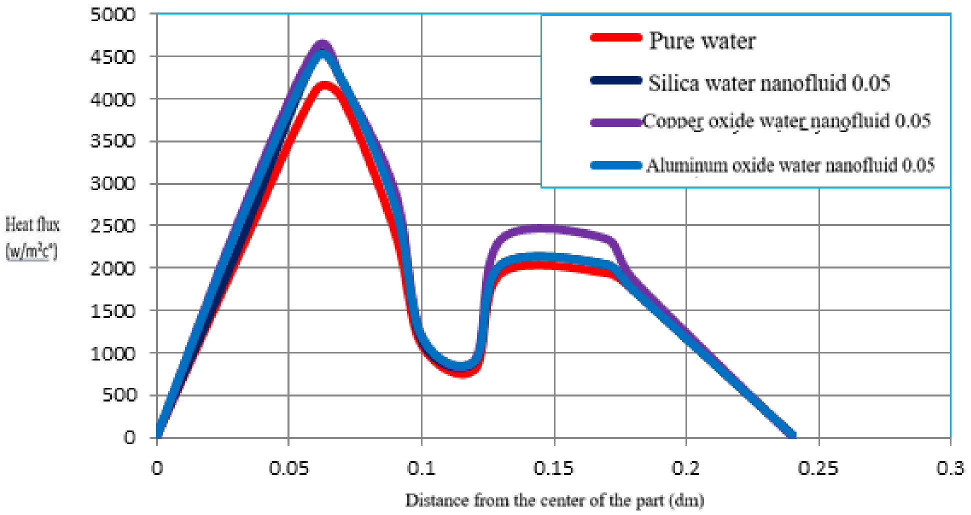

Fig. 10 Heat flux for 0.15% volume concentration of all nanofluids and base fluid (pure water)

8- Conclusion

In this study, the heat transfer behavior of nanofluids of silica oxide water, nanofluids of copper oxide water, nanofluids of aluminum oxide water, and pure water as the base fluid on a vertical brass cylinder was investigated through numerical simulation. The temperature changes of the center of the part were obtained. In this work, the heat transfer process is initially carried out with a faster temperature decrease than in the laboratory work. Also, at the end of the heat transfer process, the temperature drops suddenly. In this study, the effect of varying the size of different nanoparticles, including silica, copper, and aluminum oxide, on heat transfer on a brass cylinder was investigated in simulation. The results showed that the presence of nanoparticles with higher thermal conductivity increased heat transfer and reduced heat transfer time, resulting in a 15% increase in heat flux. The results also showed that copper nanoparticles had better heat transfer. Also, this study has examined the effect of changing the volume fraction of nanoparticles on heat transfer on a brass cylinder. The results show that increasing the volume fraction of nanofluid increases heat transfer and reduces heat transfer time, and thus increases the transfer coefficient by up to 38% compared to pure water. The results of this section show that volume fractions greater than (0.05) increase heat transfer.

The general results of this paper can be summarized as follows:

1- The cooling curve of the cylinder in pure water and nanofluid have similar behavior
2- Adding nanofluid to the base fluid increases the heat flux of all volume fractions compared to pure water, and the highest increase in heat flux is 15% at a volume fraction of 0.15%.
3- By increasing the volume fraction of nanofluid (0.15), the heat transfer time decreases
4- Based on the results, the water-copper oxide nanofluid at a concentration of 0.15 showed the greatest increase in heat transfer, which is consistent with the higher thermal conductivity of copper nanoparticles.

References

[1] Ghanbaral, S,. Numerical study of the effect of using water-aluminum oxide and water-copper nanofluids on heat transfer in a shell-and-tube heat exchanger. *International Conference on Heat Exchanger*, 2011, 3.

[2] Coursey, J. S., & Kim, J. (2008). Nanofluid boiling: The effect of surface wettability. *International Journal of Heat and Fluid Flow*, *29*(6), 1577-1585.

[3] Kim, H., DeWitt, G., McKrell, T., Buongiorno, J., & Hu, L. W. (2009). On the quenching of steel and zircaloy spheres in water-based nanofluids with alumina, silica and diamond nanoparticles. *International Journal of Multiphase Flow*, *35*(5), 427-438.

[4] Jahanshahi, M., Hosseinizadeh, S. F., Alipanah, M., Dehghani, A., & Vakilinejad, G. R. (2010). Numerical simulation of free convection based on experimental measured conductivity in a square cavity using Water/SiO2 nanofluid. *International communications in heat and mass transfer*, *37*(6), 687-694.

[5] Ranjan, A., Priy, A., Ahmad, I., Pathak, M., Khan, M. K., & Keshri, A. K. (2023). Heat transfer characteristics of pool boiling with scalable plasma-sprayed aluminum coatings. *Langmuir*, *39*(18), 6337-6354.

[6] Fadhala, G. M., & Hameed, H. G. (2025). Improving heat transfer in pool boiling: a review of surface modifications on horizontal tubes. *Journal of Thermal Analysis and Calorimetry*, *150*(16), 12045-12062.

[7] Ali, B. M. (2024). An experimental study of heat transfer in pool boiling to investigate the effect of surface roughness on critical heat flux. *ChemEngineering*, *8*(2), 44.

[8] Pakravan, H. A., & Yaghoubi, M. (2013). Analysis of nanoparticles migration on natural convective heat transfer of nanofluids. *International Journal of Thermal Sciences*, *68*, 79-93.

[9] Amiri, A., Shanbedi, M., Amiri, H., Heris, S. Z., Kazi, S. N., Chew, B. T., & Eshghi, H. (2014). Pool boiling heat transfer of

CNT/water nanofluids. *Applied Thermal Engineering*, *71*(1), 450-459.

[10] Kazem, M., Vahid Monfared, V., Daneshmand, S., & Davoudi, A. (2021). Numerical Simulation on Heat Transfer of Nanofluid in Conical Spiral Heat Exchanger. *Progress in Computational Fluid Dynamics, An International Journal* 21, 52.

[11] SA, M. N., & Hassan, A. (2023). A review of pool boiling heat transfer properties by nanofluid. *Jurnal Teknologi (Sciences & Engineering)*, *85*(3), 1-13.

[12] Abdolvand, R., Yoosefzadeh, S., Jaffar, H. A., Abdul-Redha, H. K., Akbari, O. A., Ahmadi, G., ... & Pirmoradian, M. (2025). Numerical simulation of combined convective heat transfer in a sinusoidal cavity with lid-driven cap affected by fractal blocks. *International Journal of Thermofluids*, *26*, 101048.

[13] Daneshmand, S., Adelnia, R., & Aghanajafi, C. (2008). The effect of layer thickness on aerodynamic characteristics of wind tunnel RP models. *Journal of Fluid Science and Technology*, *3*(1), 22-30.

[14] Masuda, H., Ebata, A., & Teramae, K. (1993). Alteration of thermal conductivity and viscosity of liquid by dispersing ultra-fine particles. Dispersion of Al2O3, SiO2 and TiO2 ultra-fine particles.

[15] Ahmed, S. E., Hussein, A. K., Mansour, M. A., Raizah, Z. A., & Zhang, X. (2018). MHD mixed convection in trapezoidal enclosures filled with micropolar nanofluids. *Nanoscience and Technology: An International Journal*, *9*(4).

[16] Bolukbasi, A., & Ciloglu, D. (2011). Pool boiling heat transfer characteristics of vertical cylinder quenched by SiO2–water nanofluids. *International Journal of Thermal Sciences*, *50*(6), 1013-1021.